HHS Public Access

Author manuscript

Aerosol Sci Technol. Author manuscript; available in PMC 2015 December 21.

Published in final edited form as:

Aerosol Sci Technol. 2012 ; 46(8): 897–904. doi:10.1080/02786826.2012.680551.

Design Optimization of a Portable Thermophoretic Precipitator Nanoparticle Sampler

Art Miller[1], **Alek Marinos**[1], **Chris Wendel**[1], **Grant King**[1], and **Aleksandar Bugarski**[2]

[1]National Institute for Occupational Safety and Health, Spokane, Washington, USA

[2]National Institute for Occupational Safety and Health, Pittsburgh, Pennsylvania, USA

Abstract

Researchers at the National Institute for Occupational Safety and Health (NIOSH) are developing methods for characterizing diesel particulate matter in mines. Introduction of novel engine and exhaust after treatment technologies in underground mines is changing the nature of diesel emissions, and metrics alternative to the traditional mass-based measurements are being investigated with respect to their ability to capture changes in the properties of diesel aerosols. The emphasis is given to metrics based on measurement of number and surface area concentrations, but analysis of collected particles using electron microscopy (EM) is also employed for detailed particle characterization. To collect samples for EM analysis at remote workplaces, including mining and manufacturing facilities, NIOSH is developing portable particle samplers capable of collecting airborne nano-scale particles. This paper describes the design, construction, and testing of a prototype thermophoretic precipitator (TP) particle sampler optimized for collection of particles in the size range of 1–300 nm. The device comprises heated and cooled metal plates separated by a 0.8 mm channel through which aerosol is drawn by a pump. It weighs about 2 kg, has a total footprint of 27 × 22 cm, and the collection plate size is approximately 4 × 8 cm. Low power consumption and enhanced portability were achieved by using moderate flow rates (50–150 cm^3/min) and temperature gradients (10–50 K/mm with ΔT between 8 K and 40 K). The collection efficiency of the prototype, measured with a condensation particle counter using laboratory-generated polydisperse submicrometer NaCl aerosols, ranged from 14–99%, depending on temperature gradient and flow rate. Analysis of transmission electron microscopy images of samples collected with the TP confirmed that the size distributions of collected particles determined using EM are in good agreement with those determined using a Fast Mobility Particle Sizer.

Address correspondence to Art Miller, National Institute for Occupational Safety and Health, Spokane Research Lab, 315 E. Montgomery Ave, Spokane, WA 99207, USA. ALMiller@cdc.gov.

INTRODUCTION

The National Institute for Occupational Safety and Health (NIOSH) is conducting research on the characterization and mitigation of hazardous airborne pollutants in underground mines, including nano-scale diesel aerosols. Directing the research focus toward the characterization of nano-aerosols in workplace environments is motivated by the realization that bioavailability and potential toxicity of nano and ultrafine materials is higher than that of fine materials (Oberdoerster 2001; Cardello et al. 2002; Ibald-Mulli et al. 2002; Kandlikar et al. 2007).Much of the health-motivated research is focused on measuring the number, size, and surface area of airborne particles in the workplace, in addition to their mass concentration, which is more commonly measured. Additionally, there is a need for more detailed characterization of the morphology and chemical composition of airborne nanoparticles (Oberdoerster et al. 2005; Balbus et al. 2007).

To characterize workplace aerosols, spot samples are often collected for subsequent detailed analysis by techniques including transmission electron microscopy (TEM), scanning electron microscopy (SEM), and energy dispersive spectroscopy (EDS). In order to individually characterize airborne particles using electron microscopy (EM) methods, the particles must be collected on special substrates for insertion into the electron microscope. Methods of collecting particles onto substrates for microscopy include those employing inertial impaction, gravitational settling, vapor deposition, and electrostatic precipitation (Miller et al. 2008). An alternative to these methods is a method based on thermophoretic deposition.

Particle samplers based on thermophoretic deposition were used extensively in the past for collecting respirable particles in mines (Watson 1937; Orr and Martin 1958) before being replaced by the more popular aerodynamic methods. They offer the advantage of providing low particle velocities (Thomassen et al. 2006), especially useful for gentle collection of complex agglomerated particles onto the sample substrate, and have the added advantage that even the smallest of nanoparticles are effectively collected. The latter is driving renewed interest in thermophoretic methods, for use in the collection and analysis of nanoparticles.

Thermophoretic deposition of particles occurs when there is a temperature difference across the aerosol flow field (Figure 1). As particles with linear velocity V_x encounter the temperature gradient, the increased kinetic energy of gas molecules striking the particles from the high-temperature region causes the particles to drift toward the cooler region at a velocity V_{th} (Equation (1)) determined by the thermophoretic force (Hinds 1999).

It has been shown that the magnitude of V_{th} is size- and mass-independent for particles in the free molecular regime where Knudsen number (Kn) is much greater than unity (Brock 1962) and nearly so for particles in the transition regime ($Kn \approx 1$) (Lorenzo et al. 2007). Note that for a 100-nm particle in ambient air, $Kn = 1.32$, suggesting that thermophoretics can be used for collecting nanoparticles without size bias. The thermophoretic force and the resulting thermophoretic velocity of particles have been quantified by various authors, most

notably by Epstein (1929), Brock (1962), and Talbot et al. (1980). The equation most commonly used to describe this velocity (Talbot et al. 1980) is:

$$V_{th}=\frac{-K_{th}\upsilon_g\nabla T}{T_p} \quad [1]$$

where

$$K_{th}=2C_s\frac{(k^*+C_tKn)C_c}{(1+2C_mKn)(1+2k^*+2C_tKn)} \quad [2]$$

In Equation (1), the negative convention is used to show that the velocity is in the direction of decreasing temperature. K_{th} is the thermophoretic coefficient, ν_g is the kinematic viscosity of the gas, ∇T is the temperature gradient, and T_p is the temperature of the particle (assumed to be the ambient sampling temperature if no preheating is done to the air that is sampled). In Equation (2), C_s is the thermal slip coefficient, C_t is the temperature jump coefficient, C_c is the Cunningham slip correction factor, C_m is the momentum exchange coefficient, and $k^* = k_g/k_p$, where k_g and k_p are thermal conductivities of the gas and the particles, respectively. Based on earlier empirical work, the chosen values for C_s, C_t, and C_m used in this study were 1.17, 2.18, and 1.146, respectively (Talbot et al. 1980).

The Cunningham slip coefficient (C_c) makes a correction for particles outside the continuum regime, i.e., with $Kn \approx 1$ or $Kn >> 1$, where the drag force is less than that predicted by Stokes' law. The formula of coefficient for particles in air (Davies 1945) is:

$$C_c=1+Kn\cdot\left[1.257+0.4\cdot\exp\left(-\frac{1.1}{Kn}\right)\right] \quad [3]$$

Previous thermophoretic precipitators (TPs) have been successfully used for collection of particles with diameters between 15 nm and 300 nm without shape or composition bias (Lorenzo et al. 2007). This lack of bias is important for collection of representative samples of nano-aerosols for EM analysis as it facilitates the generation of an accurate particle size distribution from a relatively small number of imaged particles.

The use of TP particle samplers is not new. One of the first TP samplers was constructed by Green and Watson (Watson 1937). Their device used a wire-to-plate design and had 2 glass slips spaced 0.5 mm apart with a heated wire between them. In such a TP, the wire heats easily but has the disadvantage of creating an asymmetrical temperature field if the plate below the wire is relatively wide. The temperature gradient will be strong near the smallest perpendicular distance from the wire but will decrease significantly with radial distance from it. Most recently developed TPs have therefore used a plate-to-plate design (Tsai and Lu 1995; Messerer et al. 2003; Lorenzo et al. 2007). Published results based on these designs suggest that channel height must not be too low, that high flow rates or anomalies in flow path can cause non-uniform deposition, and that moderate temperature gradients are appropriate. Such details were further considered in this study, during the selection of design parameters.

A plate-to-plate TP entails a flow channel comprised of 2 similarly sized plates spaced apart at a fixed height, each at a constant (but different) temperature, resulting in a uniform temperature gradient at every location between the plates. This is preferable because a symmetric and stable temperature field allows for uniform particle deposition onto sampling media such as TEM grids and other substrates.

With the goal of designing a robust, field-portable, plate-to-plate TP sampler for use in collecting nanoparticle samples for subsequent EM and microanalyses, a prototype TP sampler was designed, built, and tested. Design criteria for the prototype included minimal power consumption, high collection efficiency (greater than 95%) onto metallic plate media, accommodation for both TEM and SEM sampling, and reasonable (minimized) collection times. This paper describes the process of designing, building, and testing the prototype TP sampler.

SELECTION OF DESIGN PARAMETERS

Portability was the primary driver in developing preliminary designs for the prototype TP and led to design choices that minimized power consumption, since battery size and weight would eventually be a key factor in determining portability. These choices included using ambient air for cooling and a relatively small temperature differential provided by a resistance heater. Another preliminary design choice was the use of a metallic plate as the sample collection medium, with no dimension larger than approximately 75 mm, so that it could fit into most SEM sample chambers. A means of inserting and removing the sample media was needed that was simple for the user while maintaining a sealed flow channel. The media also needed to incorporate the option for TEM sampling by allowing the mounting of TEM grids onto the sample plate. Finally, the sampler was required to draw at least 50 cm^3/min of aerosol during operation to minimize potential diffusion losses of the smaller nanoparticles in the inlet due to long residence times. The prototype TP sampler design was preceded by designing and testing a laboratory testbed, used to evaluate design parameters including temperature gradient, channel geometry (height, width, and length), and aerosol flow rate. The ranges for these parameters were selected based on previously published data and engineering design considerations as detailed in the following paragraphs.

The first parameter that was addressed was channel height, or gap between the plates. Channel height affects the flow and particle residence time, the magnitude of the temperature gradient, and thereby the distance required for particles to travel before being deposited on the collection medium. Of the papers reviewed, previously developed plate-to-plate TPs have incorporated channel heights between 0.15 mm (Maynard 1995) and 1.45 mm (Messerer et al. 2003). Smaller heights reduce the number of particles entering the collection region for a given velocity, and can present fabrication challenges in maintaining uniform planar surfaces to achieve a uniform flow field and temperature gradient. A small channel height also magnifies the effects of any potential flow anomalies caused by surface roughness, topography, or small defects due to fabrication and assembly of parts, most notably at the leading edge of the channel. Based on these considerations and data from the literature, a preliminary channel height of 0.8 mm was selected.

The flow channel width was next addressed, accounting for the desired flow rate and the minimization of possible edge effects along the side walls. The channel cross section and flow rate affect the Reynolds number, which needs to be sufficiently low so that laminar flow is maintained to prevent turbulent mixing and vertical re-entrainment of particles. A small channel width could amplify edge effects such as eddies that disturb the laminarity of the flow, while a large channel width has the downside that it increases the required area of the heated plate and thus increases power consumption. Reviewed publications list channel widths as large as 80 mm (Maynard 1995) and as small as 3 mm, i.e., the width of a standard TEM grid (Wen and Wexler 2007). In an effort to reduce edge effects on particle collection and limit power consumption yet maintain reasonable flow rates, a channel width of 20 mm was selected for the preliminary design.

The next parameter considered was the temperature difference (ΔT) between the plates. With the channel height (h) set, the temperature gradient (∇T) is directly proportional to ΔT ($\nabla T = \Delta T/h$). The goal was to minimize the temperature difference in order to reduce power consumption. Previous publications have reported successful TPs with a temperature gradient of up to 1000 K/mm(Maynard 1995) and as low as 13 K/mm (Messerer et al. 2003).A low temperature gradient may require a lower flow rate resulting in increased sampling time to achieve adequate particle deposition density for EM; however, some published data suggest that lower temperature gradients can be successful (Tsai and Lu 1995; Messerer et al. 2003), allowing for reduced power consumption.

While the temperature gradients vary significantly among the previously designed TPs, the temperature difference between the hot and cold plate is usually below 150°C (Maynard 1995; Gonzalez et al. 2005; Lorenzo et al. 2007). Reducing the upper temperature limit reduces the potential for thermally induced flow anomalies as well as possible alteration of particles due to their potential temperature sensitivity (Maynard 1995). Conversely, lowering the temperature of the cold plate may increase the possibility of condensation, which, with the possible exception of some bioaerosols, can adversely affect the sample. The above considerations led to a preliminary design that targeted a temperature gradient of 37.5 K/mm with an absolute temperature difference of approximately 30 K and a cold plate temperature near ambient temperature (approximately 22°C). It is clear that collection efficiency is affected by all of these parameters, and thus before proceeding, a theoretical analysis was performed to predict the effects on efficiency of the various parameters under a variety of operating conditions.

Using the selected channel geometry and temperature difference as a starting point, calculations were done using Equations (1–4) to evaluate the choices that were made and further investigate suitable operating ranges for flow rate and deposition length (Figure 2). Equation (1) was used to calculate how deposition length is affected by varying the flow rate and channel height, assuming the selected channel width of 20 mm, ΔT of 30 K, and a particle diameter of 300 nm. The deposition length was calculated with the worst case scenario in mind – that is, the distance required for a relatively large (300 nm) particle entering the collection region near the hot plate to travel downward to the cold plate. The deposition length was calculated using the ratio of the flow velocity and the thermophoretic velocity (Equation (4)).

$$l = h\frac{V_x}{V_{th}} \quad [4]$$

All particles smaller than 300 nm are expected to have a similar thermophoretic velocity and will therefore precipitate in a similar deposition length. This assumes that all particles less than 300 nm in diameter are affected by a similar thermophoretic force as suggested in previous studies (Lorenzo et al. 2007). Calculations using Equations (1–4) indicated that the thermophoretic velocity of the particles in the range of concern (1–300 nm), is expected to vary by only about 10%, which suggests that deposition will be relatively homogeneous for particles in that range and collected nanoparticle samples will therefore be representative of the target aerosol. Figure 2 provides a resource for determining the deposition length and flow rate parameters, as discussed in further detail below.

Calculations show that the deposition length increases as channel height or flow rate increases. Increasing the channel height decreases the strength of the thermal gradient, and increasing the flow rate increases the velocity of particles in the flow direction, both of which flatten the trajectory of the particles. Based on this preliminary assessment, a flow rate around 50–100 cm^3/min is desirable for the parameters selected. When a channel height of 0.8 mm is used along with a flow rate of 50–100 cm^3/min, the deposition length is expected to be about 30–60 mm, which satisfies the required 75-mm collection plate size for compatibility with SEM analysis.

LABORATORY TESTBED

After selecting the channel dimensions, a testbed was designed and built to gather preliminary data on the accuracy of the predictions. The parameters chosen for the testbed included a lower absolute temperature and channel height than the TPs cited in the literature, resulting in a lower temperature gradient. Nevertheless, high efficiency and uniform collection were still expected from this device since the calculated deposition length was shown to be less than the selected collection plate length. A series of experiments were conducted with the testbed to verify the efficiency of the sampling device given a range of flow rates and temperature differences. Additionally, a sample was collected for SEM analysis to determine if the particle deposition was uniform over the entire deposition length.

The testbed consisted of thin metallic hot and cold plates separated by insulating shims to create the flow channel. An electric resistive heater was adhered to the non-flow side of the hot plate and covered by an insulating block to increase the temperature of the hot plate and provide structure to the thin hot plate. An aluminum block with a water flow cavity was attached to the cold plate to provide structure as well as allow for temperature control via throughput of cool water. The insulating and aluminum blocks provided a surface on which to attach manifolds for the inlet and outlet flow from the sampling channel. The manifolds accepted a tube with aerosol flow and smoothly transitioned to a cross section more similar to the channel geometry to reduce turbulence. The sampling channel was designed with a

length of 150 mm such that 100% particle collection would be achieved for most cases and the deposition length could be revealed by SEM analysis.

Testbed Setup and Testing

An experimental setup was used to measure the efficiency of the testbed (Figure 3). A relatively high concentration (10^6 particles/cm^3) of NaCl aerosol was generated using a 4 mg/L NaCl solution in an atomizer, followed by a silica drier. That process generated a polydisperse aerosol of lognormal particle size distribution with a geometric mean mobility diameter near 100 nm, appropriate for evaluating the performance of the TP sampler for particles in the range below 300 nm. A 3-way valve upstream of the testbed precipitator was used to direct the flow as desired, through either the testbed or a bypass (Touloukian et al. 1971; Messerer et al. 2003). A Fast Mobility Particle Sizer (TSI FMPS 3091) was used to measure concentrations and size distributions of the dried aerosols in the range of 5.6–560 nm downstream of the precipitator testbed, and the measurements were used to determine collection efficiency of the TP.

Efficiency tests were performed by setting the precipitator at the desired flow rate and temperature difference with flow directed through the bypass channel and then switching the flow to pass through the TP testbed. After a collection period of approximately 5 min, when the number concentration had remained stable at its lowest value, the flow was again switched to the bypass channel. These trials were repeated at multiple flow rates, each with 4 temperature differences including a “null” test, where the precipitator was run with both plates at 22°C (ΔT = 0 K) to estimate the diffusion losses in the inlet, TP, and outlet tubing. Particle concentrations used to determine efficiency were calculated as the average of data collected for at least 1 min under the conditions of interest. For all tests, plate temperature was measured with thermocouples attached at the centers of the heating and cooling plates, placed on the non-flow side to eliminate flow disturbance.

Testbed Test Results

For each of the trials performed on the testbed, the total (gross) efficiency, η_T, was calculated as:

$$\eta_T = \frac{C - C_{TP}}{C} \quad [5]$$

where C is the particle concentration as measured by the FMPS when flow is through the bypass channel and C_{TP} is the concentration measured when flow is through the TP. The thermophoretic efficiency for each trial is calculated as:

$$\eta = 1 - \frac{1 - \eta_T}{1 - \eta_L} \quad [6]$$

where η_L is defined as the efficiency found during the null test when ΔT = 0 K (Tsai and Lu 1995).

Results show that the efficiency tends to increase as flow rate decreases or ΔT increases (Figure 4) and that the efficiency drops asymptotically when the flow rate increases or when the temperature gradient is decreased.

While Equations (1)–(3) predict a slight decrease in V_{th} for larger particles, the difference is less than 10% in the size range 1–300 nm. Since the residence time in the channel is relatively long, this small difference leads to a measurable size-dependent collection efficiency between the inlet and exit when ΔT is small. To elucidate this, the FMPS data were used to calculate size-dependent collection efficiency for 2 tests (Figure 5). Results show that for the higher ΔT (27K), the size-dependent difference in V_{th} does not lead to reduced collection efficiency, since the V_{th} is high relative to the residence time. However, at ΔT of 17 K, the size-dependent reduction in V_{th} does lead to size-dependent collection efficiency. Equations (1)–(3) predict that this effect would be stronger for larger particles, since V_{th} increases significantly.

A sample was collected for EM analysis using the optimum flow rate and temperature gradient. Choice of these parameters took into account the desired operating specifications of high efficiency, high flow rate to ensure reasonable sampling times, and low temperature difference to minimize power consumption. The parameters chosen for the sample to be analyzed by EM were a flow rate of 75 cm^3/min and a temperature difference of 27 K (34 K/mm), which resulted in a thermophoretic efficiency greater than 95%. SEM images were obtained from a sample collected using the chosen parameters (13 min, ΔT = 27 K, Q = 75 cm^3/min) and were used for a qualitative analysis of the particle deposition on the sampling medium. Images from several points along the flow path at the center and edges of the collection plate revealed negligible edge effects, good particle distribution with no visible swirling or flow disturbances, and most of the particle collection occurring in the first 50–75 mm of the collection region.

DESIGN AND TESTING OF THE PROTOTYPE TP

Results from the testbed were used to design and build the first-generation TP prototype. Based on testbed results, several design changes were implemented to reduce power consumption, increase collection efficiency, and facilitate further testing.

The first design change was shortening the length of the sample plate from 152 mm to 76 mm, since from the testbed SEM analysis, it was clear that for most cases the particles were deposited in the first half of the plate as predicted by the parametric study. Next, to allow for forced air convection cooling, the bottom block was designed of aluminum with 25 holes drilled through it for air passage, to maintain the sample plate near ambient temperature. Finally, adapting the flow from a small-diameter tube to the much different channel geometry was done using a plenum just upstream of the sampling channel that was large relative to the flow cross section. This decreased the velocity of the flow from the inlet delivery tube by a factor of approximately 15 before reaching the channel inlet, to eliminate inlet turbulence and to distribute the flow across the width of the channel to avoid increased deposition along the centerline as evidenced in previous work (Thayer et al. 2011).

Prototype TP – Parameters and Description

Based on the results of the parametric study and testbed evaluation, a prototype was designed and constructed. The device weighs about 2 kg (excluding the cooling pump) and has a footprint of 27 × 22 cm including the power supply, sampling pump, and thermocouple reader. The inlet, outlet, and top block (central housing) have a footprint of 9 × 12 cm (Figure 6) and are made from chlorinated polyvinyl chloride (CPVC) because of its insulating properties and relatively high melting temperature, while aluminum (6061) is used for the bottom block to improve thermal conductivity. The hot plate and sample plate are approximately 4 × 8 cm in size and made of copper sheet metal because of its high thermal conductivity. The flow-side of both copper plates is mirror finished to eliminate flow disturbances, reduce the emissivity, and increase SEM image quality (since the cold plate is inserted directly into the SEM for sample analysis).

The sampling plate is attached to a circular sample holder that can be easily inserted and removed from the central housing (Figure 6), with airtight seal of the sample holder provided by an O-ring. A 0.13-mm-deep, 3.18-mm-diameter recess in the plate, able to accommodate a standard TEM grid, is located 10 mm downstream of the leading edge of the plate. Constant channel height is maintained by use of ball detents in the top block that apply downward pressure on the edge of the sampling plate.

Thermocouples are used to monitor the hot plate and cold plate temperatures. The hot plate thermocouple is inserted between the non-flow side of the hot plate and the resistive heater. The cold plate thermocouple is recessed in a small-diameter hole drilled into the bottom block approximately 1 mm below the flow channel. The temperature of the hot plate is adjusted by changing the voltage to the heater, which is attached to the back of the hot plate with thermal contact paste. The temperature of the cold plate is maintained near room temperature (22° ± 2°C for tests described here) by drawing air through the holes in the aluminum block using a small pump.

Prototype TP Testing

An experimental setup similar to the one used to evaluate the testbed (Figure 3) was used to evaluate the prototype. The test setup was improved by including an optional bypass flow upstream of the precipitator that filters the sampling air before it reaches the precipitator. This allows for constant airflow through the precipitator, which is either clean or contains particles, depending on the upstream path of the flow. For the efficiency tests, the FMPS was replaced with a condensation particle counter (CPC, TSI Model 3007) because only the total number of particles was needed (not a size distribution).

Samples intended for image analysis were obtained by establishing a steady state temperature difference between the plates while running filtered air through the sampling channel and then switching the flow to particle-laden aerosol for a duration based on the desired particle deposition density. After the test duration, the flow was switched back to filtered air and the power to the resistive heater was turned off to allow the precipitator to cool before the sample plate was removed for EM analysis.

Prototype TP Test Results

The prototype TP was tested to determine collection efficiency, verify optimal sampling parameters based on the new channel dimensions, and study the quality of collected samples. Collection efficiency was measured using similar NaCl aerosol as with the testbed, and similar efficiency values were achieved e.g., 96% efficiency with ΔT = 19.5 K and Q = 50 cm^3/min. To avoid redundancy, those data are not presented here. The operation of the prototype was further validated using the same polydisperse NaCl aerosol used for the testbed (geometric mean diameter of approximately 100 nm) and measuring particle concentration at the exit versus the temperature difference of the plates over the course of a test and cool down cycle (Figure 7). Those data demonstrate that thermophoretic precipitation is the key deposition mechanism, showing an inverse correlation between the temperature difference and the number of particles measured by the CPC at the outlet of the TP. They also show that the particle concentration lags the temperature difference by a noticeable duration (approximately 90 s) – a result of the thermal inertia and residence time of particles within the system.

In addition to verifying collection efficiency, tests were conducted to evaluate whether the samples obtained by the prototype were representative of the aerosol being sampled. The aerosol concentration and size distribution used were similar to that expected for field applications, i.e., sampling of diesel exhaust particles. A series of samples were collected from an aerosol with concentration of 10^6 particles/cm^3 using different sampling parameters to assess which parameters led to optimal particle deposition density, as needed for the eventual EM and image analysis of diesel particles. Analysis of the samples revealed that excellent deposition and particle density could be obtained with a flow rate of 120 cm^3/min, a ΔT of 21.3 K (temperature gradient of 26.6 K/mm), and a sampling duration of 3 min. A sample was collected at these conditions and images were acquired from both the sampling plate (SEM) and the TEM grid (TEM) (Figure 8). From the SEM images, a qualitative assessment was done to determine deposition uniformity. The deposition was found to be uniform across the entire plate with minor, localized edge effects.

Image analysis was performed on TEM images taken from a TEM grid located 10 mm from the leading edge of the sample plate to investigate whether the collected samples were representative of the sample aerosol. A total of 42 images containing a total of 569 particles were taken at evenly spaced locations in a rectangular matrix pattern across the center portion of the TEM grid. ImageJ, an image-processing program developed by the National Institutes of Health (NIH), was used for image analysis. The projected surface area of each particle, A, was determined using ImageJ, and from this a projected area equivalent diameter, D_{pa}, was calculated (Equation (7)):

$$D_{pa} = \sqrt{\frac{4A}{\pi}} \quad [7]$$

The projected area diameters of the particles were combined into a particle size distribution and compared to FMPS electrical mobility diameters (D_m) obtained by measuring the average particle size distribution of the same NaCl aerosol (Figure 9). No data fitting or

correction factors were applied to the image analysis data. To account for the difference in particle concentration between the 2 data collecting methods, the FMPS data, which represent the average particle size distribution for 150 measurements taken during the sampling period, were scaled down by a factor equal to the ratio of the peak heights.

The image analysis data and FMPS data correlate well considering the relatively small (but adequate) number of particles used for the image analysis. Both curves are lognormal and have peaks near 100 nm. The FMPS curve is smoother because it is comprised of data from about 180 million particles over a 2.5 min time period, whereas the image analysis data are from only 569 total particles. These data demonstrate that the sample is quite representative of the original aerosol.

CONCLUSION

Using data from published literature and theoretical calculations, a prototype plate-to-plate TP nanoparticle sampler was designed, constructed, and evaluated. Using the parameters ΔT = 19.5 K and Q = 50 cm^3/min, particle deposition adequate for EM analysis, and gross collection efficiency of 96% were measured for sampling of laboratory-generated NaCl aerosols during relatively short (3-min) tests. Unique features of the prototype TP sampler included air cooling of the cold plate and an easily removable substrate that can accommodate both SEM and TEM sampling. SEM images of samples showed uniform deposition with minimal edge effects and flow disturbances. A particle distribution histogram created using image analysis of TEM micrographs showed strong agreement with the size distribution measured using an FMPS.

Based on these results, NIOSH researchers are pursuing the development of a portable TP to collect nano-scale diesel emissions from equipment in mines to further understand the changes in the properties of diesel aerosols with the introduction of novel engine and exhaust aftertreatment technologies. The device will be field tested and further modified toward the eventual goal of producing a commercially viable portable TP nanoparticle sampler.

Acknowledgment

The authors would like to acknowledge the Gonzaga University Center for Engineering Design and specifically thank Carl Sunderman of NIOSH and Dr Steven Zemke of Gonzaga for their guidance to the students in fulfilling their project requirements and providing engineering insight. We also thank Patrick Moran, Tim Elder, and James Wong for their contributions as part of the student design team.

REFERENCES

Balbus JM, Maynard AD, Colvin VL, Castranova V, Daston GP, Denison RA. Meeting Report: Hazard Assessment for Nanoparticles–Report from an Interdisciplinary Workshop. Environ. Health Persp. 2007; 115:1654–1659.

Brock JR. On the Theory of Thermal Forces Acting on Aerosol Particles. J. Colloid Sci. 1962; 17:768–780.

Cardello N, Volckens J, Tolocka MP, Wiener R, Buckley TJ. Technical Note: Performance of a Personal Electrostatic Precipitator Particle Sampler. Aerosol Sci. Technol. 2002; 36:162–165.

Davies CN. Definitive Equations for the Fluid Resistance of Spheres. Proc. Phys. Soc. 1945; 57:259–270.

Epstein PS. Zur Theorie des Radiometers. Z. Phys. 1929; 54:537–563.

Gonzalez D, Nasibulin AG, Baklanov AM, Shaddakov SD, Brown DP, Queipo P, et al. A New Thermophoretic Precipitator for Collection of Nanometer-Sized Aerosol Particles. Aerosol Sci. Technol. 2005; 39:1064–1071.

Hinds, WC. Aerosol Technology. New York: John Wiley & Sons; 1999.

Ibald-Mulli A, Wichmann H-E, Kreyling W, Peters A. Epidemiological Evidence on Health Effects of Ultrafine Particles. J. Aerosol Med. 2002; 15:189–201. [PubMed: 12184869]

Kandlikar M, Ramachandran G, Maynard A, Murdock B, Toscano WA. Health Risk Assessment for Nanoparticles: A Case for Using Expert Judgment. J. Nanoparticle Res. 2007; 9:137–156.

Lorenzo R, Kaegi R, Gahrig R, Scherrer L, Grobety B, Burstscher H. A Thermophoretic Precipitator for the Representative Collection of Atmospheric Ultrafine Particles for Microscopic Analysis. Aerosol Sci. Technol. 2007; 41:934–943.

Maynard AD. The Development of a New Thermophoretic Precipitator for Scanning Transmission Electron Microscope Analysis of Ultrafine Aerosol Particles. Aerosol Sci. Technol. 1995; 23:521–533.

Messerer A, Niessner R, Pöschl U. Thermophoretic Deposition of Soot Aerosol Particles Under Experimental Conditions Relevant for Modern Diesel Engine Exhaust Gas Systems. Aerosol Sci. Technol. 2003; 34:1009–1021.

Miller, AL.; Habjan, MC.; Beers-Green, AB.; Ahlstrand, GG. A Monograph of the ACGIH® Air Sampling Instruments Committee: Microscopic Analysis of Airborne Particles and Fibers. Cincinnati, OH: ACGIH R®; 2008.

Oberdoerster G. Pulmonary Effects of Inhaled Ultrafine Particles. Int. Arch. Occup. Environ. Health. 2001; 74:1–8. [PubMed: 11196075]

Oberdoerster G, Maynard A, Donaldson K, Castranova V, Fitzpatrick J, Ausman K, et al. Principles for Characterizing the Potential Human Health Effects from Exposure to Nanomaterials: Elements of a Screening Strategy. Part. Fibre Toxicol. 2005; 2:8. [PubMed: 16209704]

Orr C, Martin RA. Thermal Precipitator for Continuous Aerosol Sampling. Rev. Sci. Instrum. 1958; 29:129.

Talbot L, Cheng RK, Schefer RW, Willis DR. Thermophoresis of Particles in a Heated Boundary Layer. J. Fluid Mech. 1980; 101:737–758.

Thayer D, Koehler KA, Marchese A, Volckens J. A Personal, Thermophoretic Sampler for Airborne Nanoparticles. Aerosol Sci. Technol. 2011; 45:744–750.

Thomassen Y, Koch W, Dunkhorst W, Ellingsen DG, Skaugset N-P, Jordbekken L, et al. Ultrafine Particles at Workplaces of a Primary Aluminum Smelter. J. Environ. Monitor. 2006; 8:127–133.

Touloukian, YS.; Powell, RW.; Ho, CY.; Klemens, PG. Thermophysical Properties of Matter: Thermal Conductivity – Nonmetallic Solids. New York: IFI/Plenum; 1971.

Tsai C-J, Lu H-C. Design and Evaluation of a Plate-to-Plate Thermophoretic Precipitator. Aerosol Sci. Technol. 1995; 22:172–180.

Watson, HH. A System for Obtaining, from Mine Air, Dust Samples for Physical, Chemical, and Petrological Examination. London: Institution of Mining and Metallurgy; 1937.

Wen J, Wexler AS. Thermophoretic Sampler and its Application in Ultrafine Particle Collection. Aerosol Sci. Technol. 2007; 41:624–629.

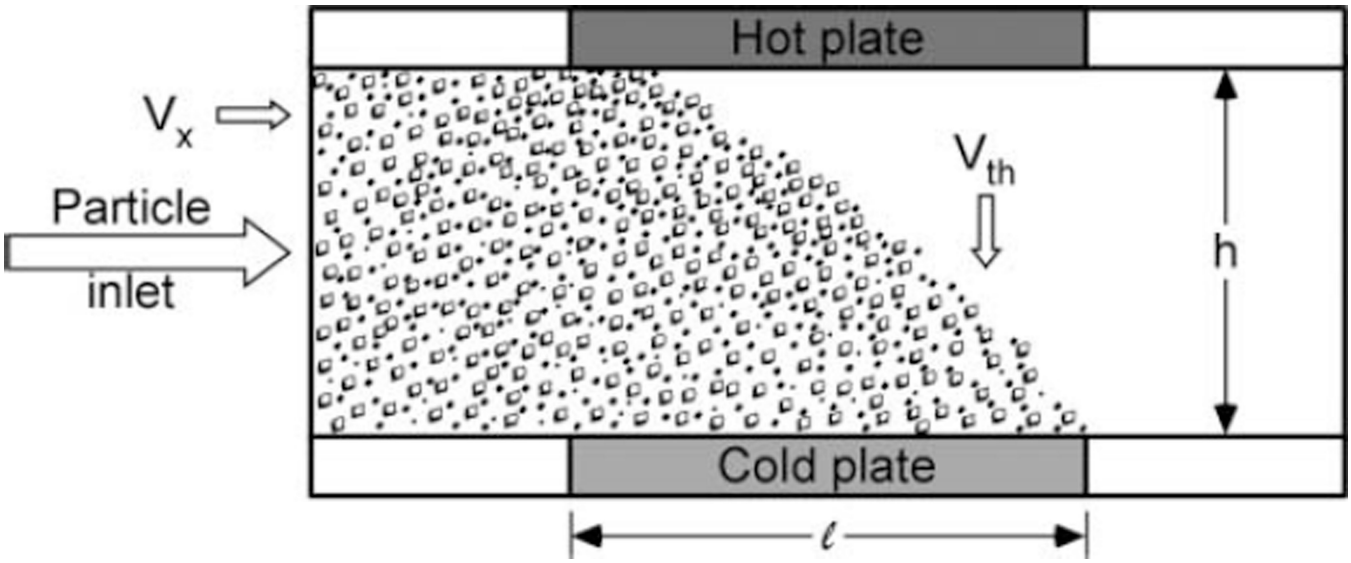

FIG. 1.

Schematic of a plate-to-plate thermophoretic precipitator channel with channel height *h* and deposition length *l*. Note that V_x is the linear velocity of the aerosol, while V_{th} is the (vertical) thermophoretic velocity of the particles

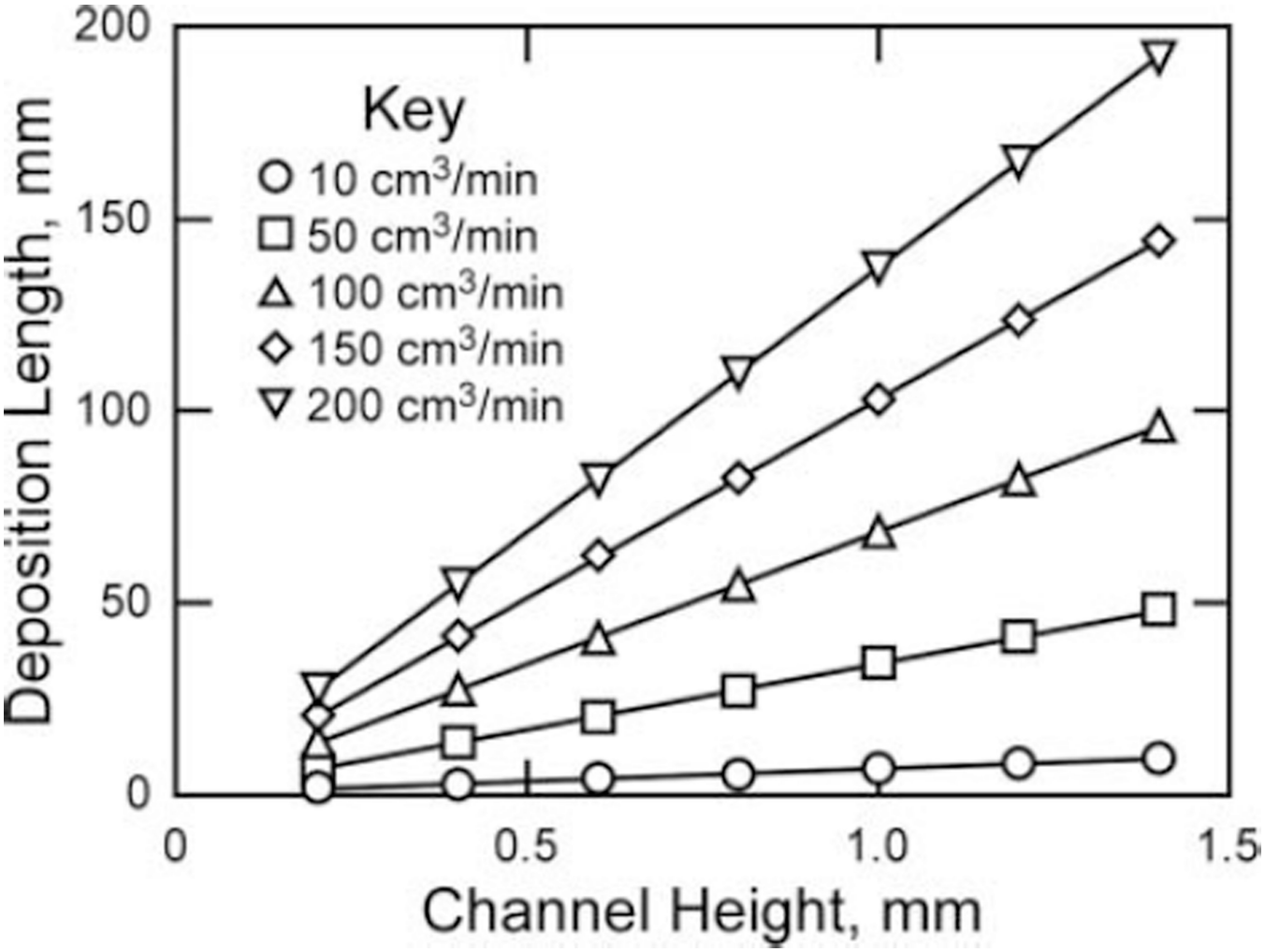

FIG. 2.

The resulting deposition length for different channel heights and flow rates with a channel width of 20 mm, Δ*T* of 30 K, and a particle diameter of 300 nm, using Equations (1–4).

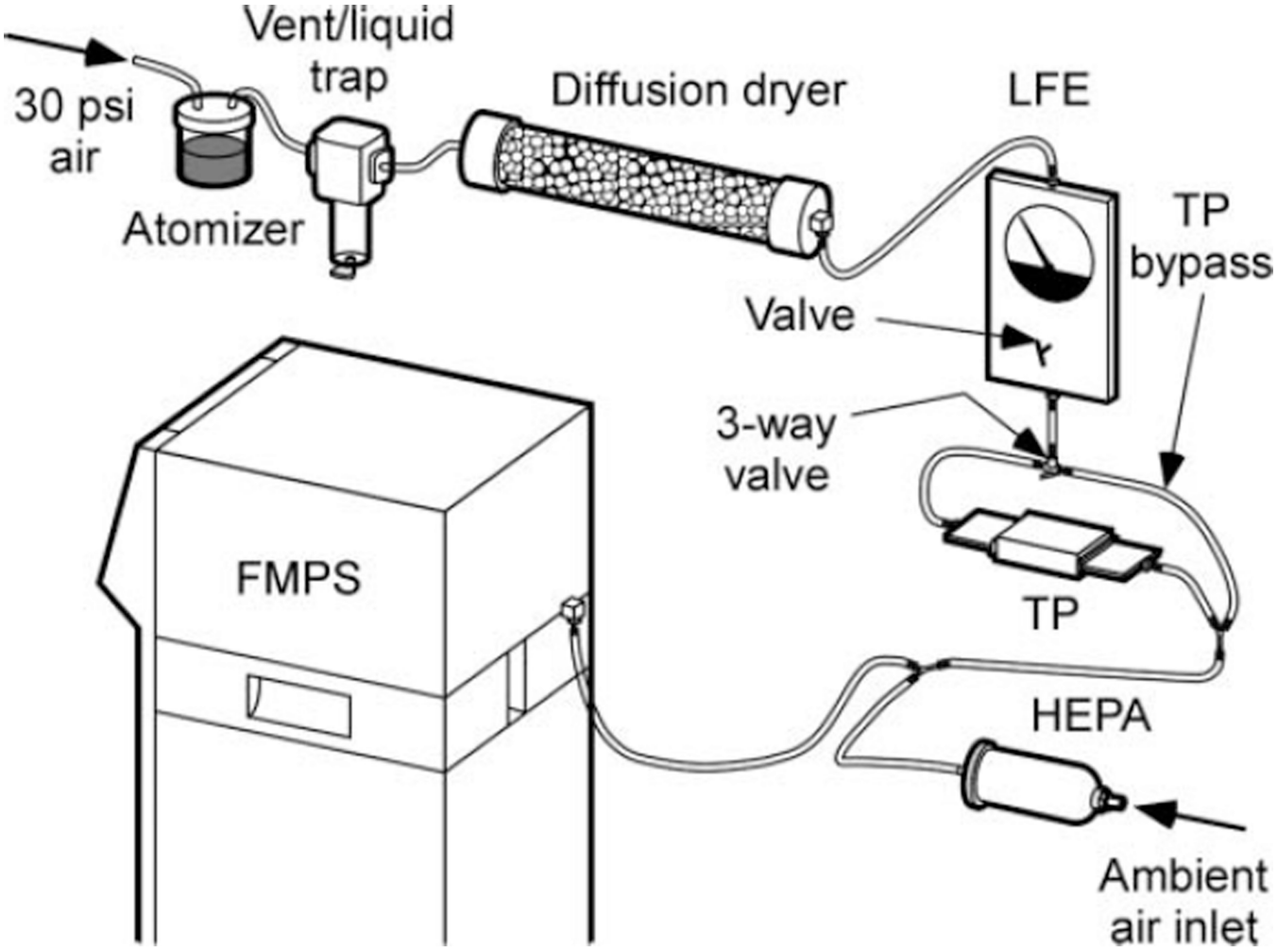

FIG. 3.

Experimental setup for testing the thermophoretic precipitator (TP) testbed, using a Fast Mobility Particle Sizer (FMPS).

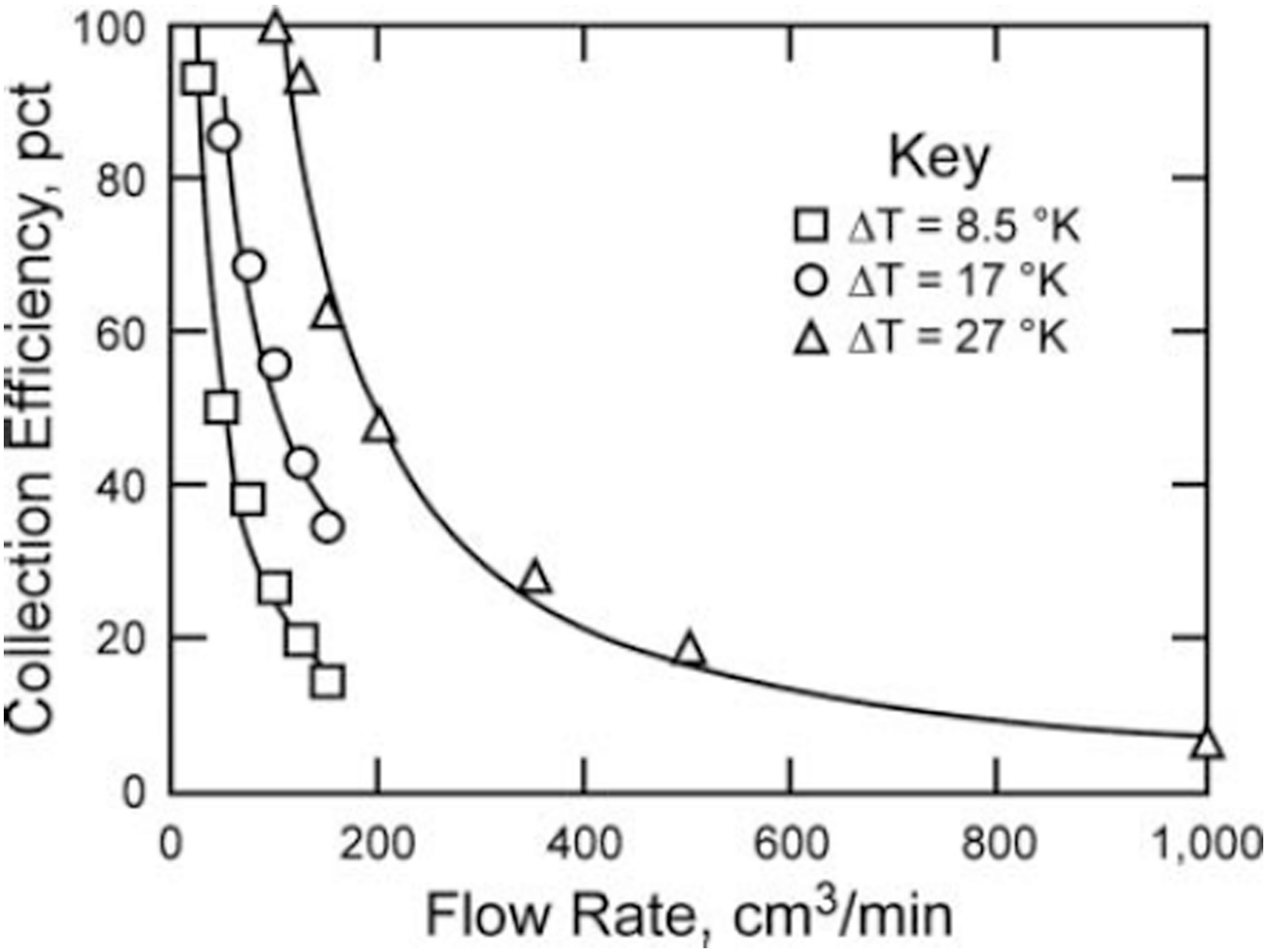

FIG. 4.

Thermophoretic collection efficiency as a function of flow rate in testbed for 3 values of Δ*T* (note that flow rates of 0–1000 cm^3/min correspond to velocities of 0–52 cm/s).

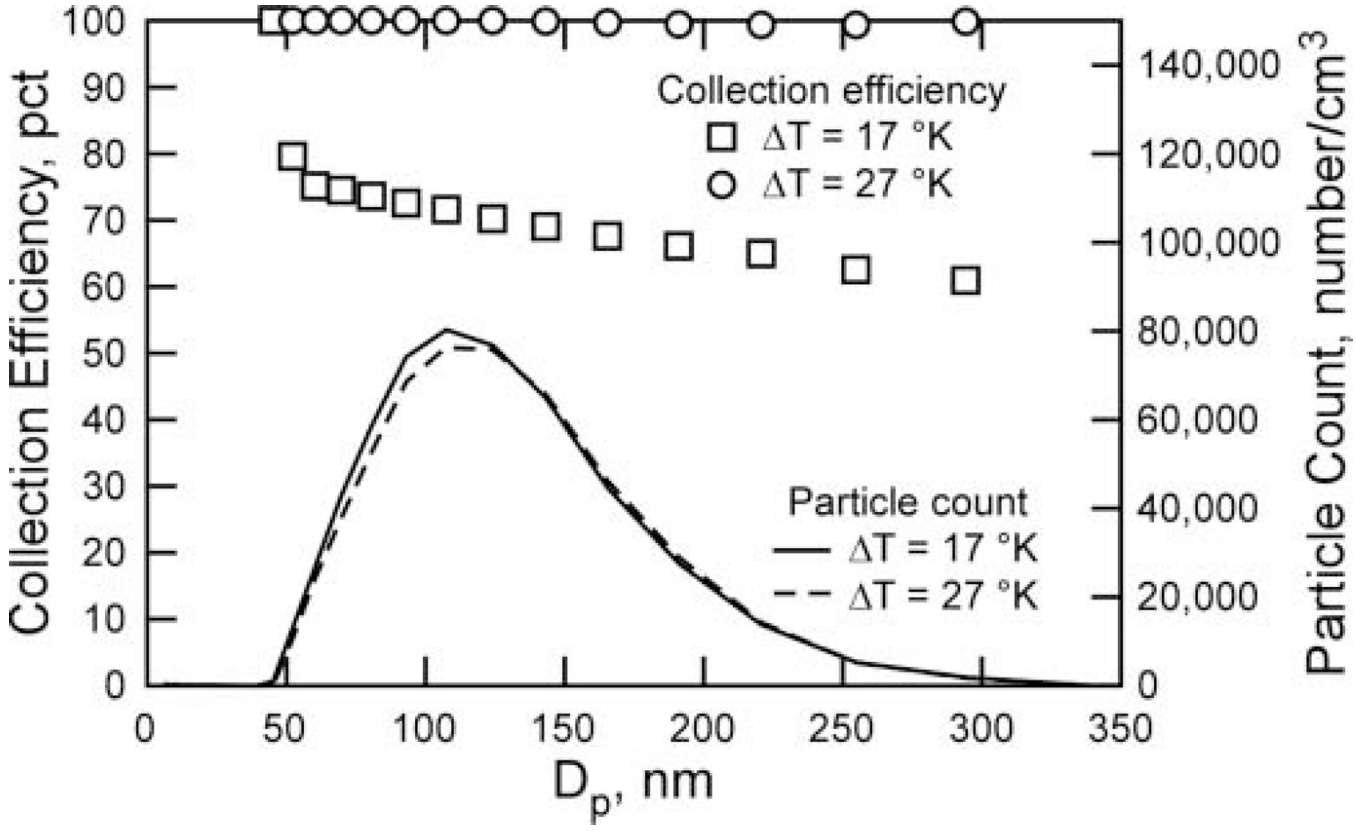

FIG. 5.

Gross collection efficiency calculated for each channel of FMPS data for 2 tests; where Δ*T* was 17 K and 27 K (note that efficiency data below 45 nm were omitted since extremely low particle numbers in that region led to undependable efficiency calculations).

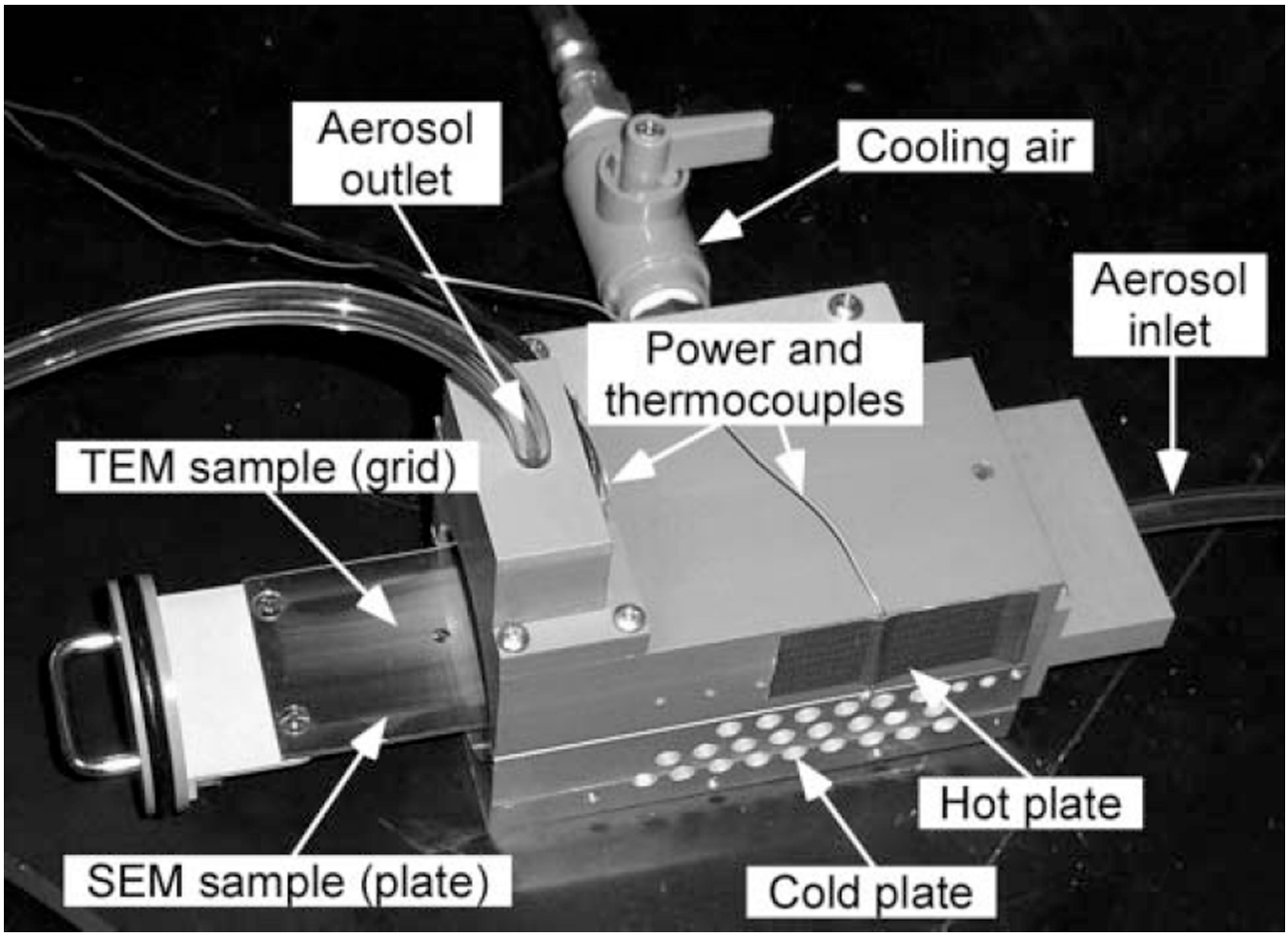

FIG. 6.
Central housing portion of the TP prototype.

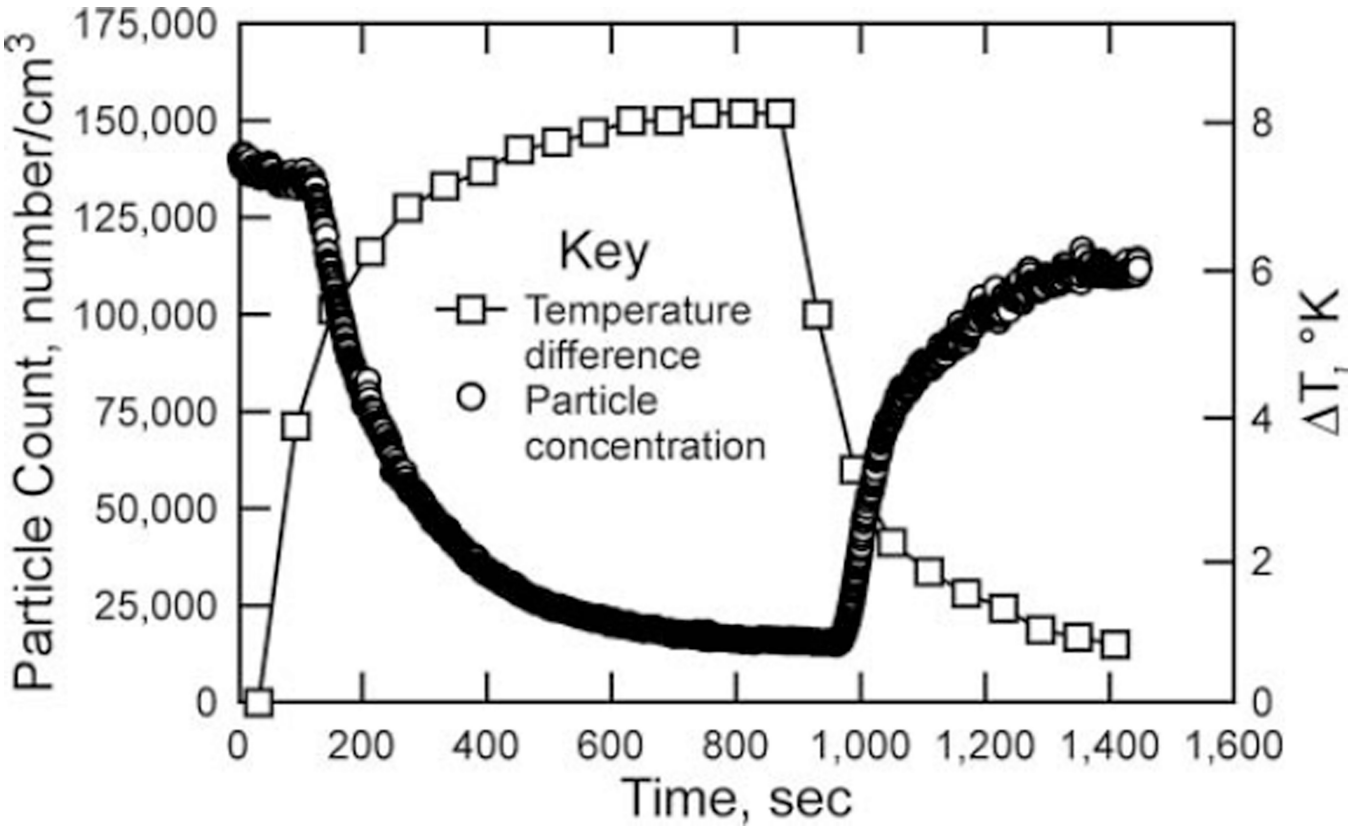

FIG. 7.

Particle concentration (measured at the TP exit) and Δ*T* for the duration of a test and cool down period, for a maximum Δ*T* of ~8 K and flow rate of 60 cm^3/min.

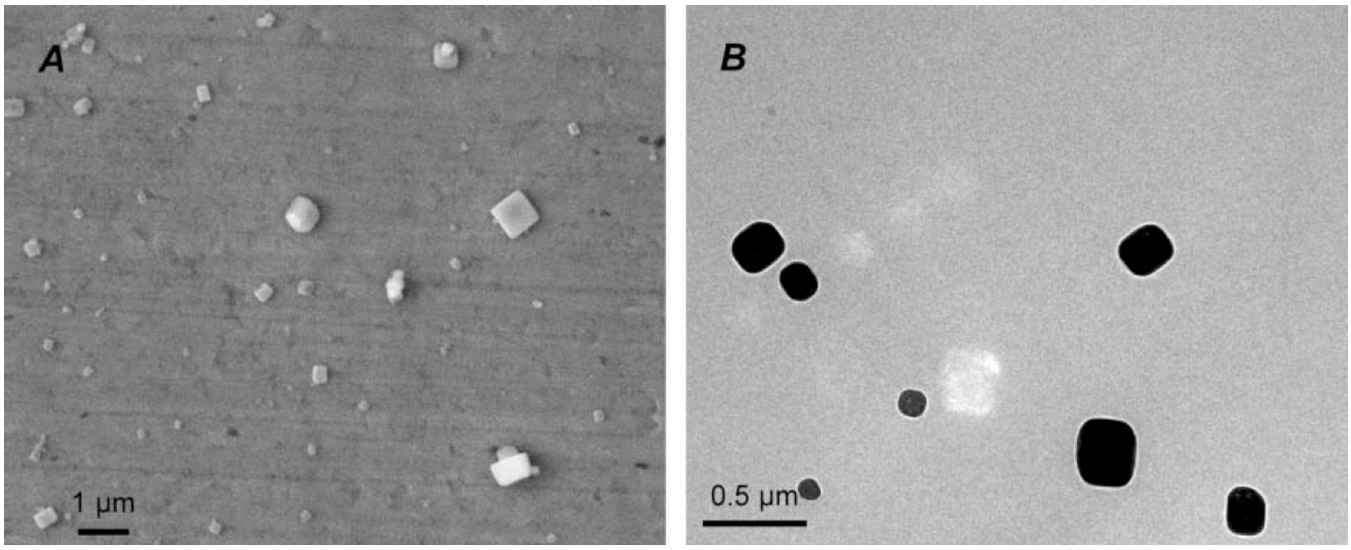

FIG. 8.

Sample EM images: (A) SEM image of NaCl particles 5 mm from the leading edge; (B) TEM image taken from a TEM grid located 10 mm from the leading edge.

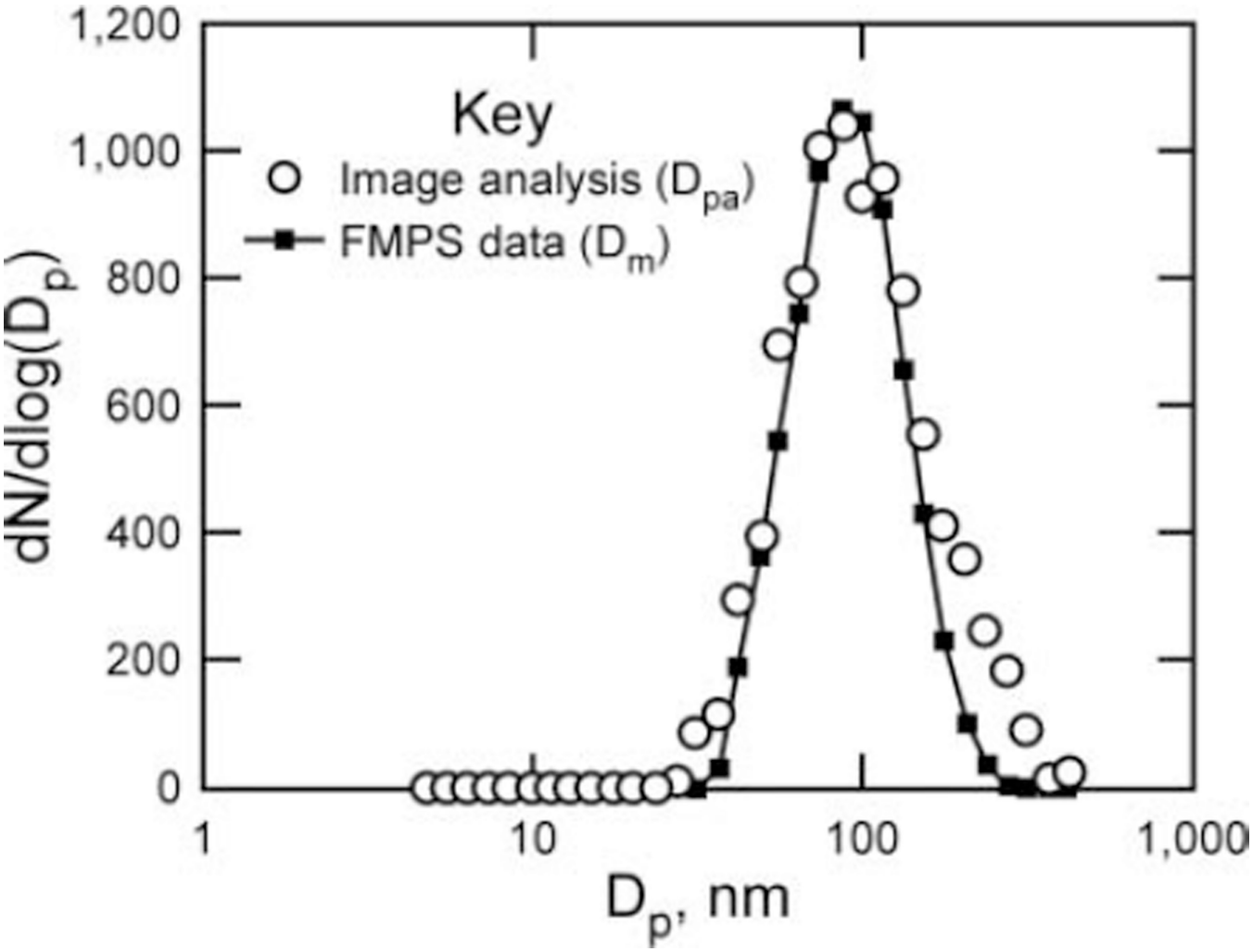

FIG. 9.
Particle size distributions from image analysis and FMPS data.